Eurasian Chemical Communications

SAMI

<u>**FULL PAPER**</u>

A computational study at blocking probability of the SARS-CoV-2 spike protein through the binding of cellular receptors

Saeedeh Mohammadi[a,b,*] |**Esmail Doustkhah**[c] | **Ahmad Reza Salehi Chaleshtori**[d] |

Mohammad Esmailpour[b] | **Farzad Zamani**[e] | **Ayoub Esmailpour**[a,*]

[a]*Department of Physics, Shahid Rajaee Teacher Training University, Lavizan, Tehran 16788-15811, Iran*

[b]*Department of Physics, Azarbaijan Shahid Madani University, Tabriz 53714-161, Iran*

[c]*International Center for Materials Nanoarchitechtonics (WPI-MANA), National Institute for Materials Science (NIMS), 1-1 Namiki, Tsukuba, Ibaraki 305-0044, Japan*

[d]*Department of Medical Genetics, Faculty of Medical Sciences, Tarbiat Modares University, P.O. Box 14115-331, Tehran, Iran*

[e]*The Institute of Scientific and Industrial Research (ISIR), Osaka University, Ibaraki-shi, Osaka 567-0047, Japan*

*Corresponding Authors:

Saeedeh Mohammadi and Ayoub Esmailpour

Email: Esmailpour@sru.ac.ir

Tel.: +98 2123322242

In this paper, the SARS-CoV-2 spike encoding gene sequences were analyzed to find the structural homology of S proteins. The S protein of SARS-CoV-2 was obtained from homology modeling and the protein-protein docking was performed to elucidate sites active in S protein for ACE2, dipeptidyl peptidase 4 (DPP4), chemokine receptor 5 (CCR5), and AXL. The two crucial binding sites of S protein, known as RBD and CTD, were investigated. Three-dimensional structures of 8 possible RBD/CTD-receptor complexes were evaluated using molecular dynamic (MD) simulations. The best simulation models of the SARS-CoV-2 S protein active sites with the receptors were obtained for the ACE2 receptor (PDB:6VW1), providing 99.5% and 98.5% coverage for CTD and RBD, respectively. The SARS-CoV-2 S protein may connect with the ACE2 receptor via the RBD sites of the S protein and the ACE2 peptidase domain (PD), which can be blocked by encoding gene sequence in the active sites of S protein, offering an attractive protection approach against this novel SARS-CoV-2 virus.

KEYWORDS

SARS-CoV-2; spike protein; homology modeling; molecular docking; dynamic simulation.

Introduction

In 2019, a highly contagious novel coronavirus appeared in China [1] and a mutated variant of the novel coronavirus in England [2] with a high rate of morbidity and mortality [3,4]. Due to the absence of efficient antiviral medication against SARS-CoV-2, the SARS-CoV-2 pandemic has soon become a global catastrophic risk to human civilization [5,6]. By end of 12 March 2021, over 118 million confirmed cases of the infection including approximately 2.6 million deaths have been globally reported [7].

The SARS-CoV-2 includes a positive-sense RNA [8,9]. The spike protein plays a key role in facilitating the viral entry into the cell [10,11].

This protein is generally split by host peptidases into two functional S1 and S2 subunits [12]. The S1 subdomain includes an NTD and a CTD, in which attaching to a host ACE2 receptor occurs via the CTD and RBD [13]. The ACE2 has a protective role in regulating the RAS, which is an endocrine that has an important responsibility to prevent lung injury in humans through controlling blood pressure and electrolyte balance [14,15]. It is known that reducing the ACE2 expression is realized via blocking the renin-angiotensin pathway [16]. Considering the importance of the S protein interactions with host receptors, therapeutic approaches with the possibility of inhibiting the protein binding

to the target receptors can be a promising pathway to block the virus entry into the human cells. Recently, we have suggested nicotine and caffeine, which bind to possible drugs for blocking S protein [17].

Although there are many ongoing reports of inhibiting SARS-CoV-2, the interaction between the cites active, *e.g.,* RBD and CTD, of the virus with target cellular receptors such as ACE2, dipeptidyl peptidase 4 (DPP4), chemokine receptor 5 (CCR5), and AXL through homology modeling has not yet been investigated. To pursue our investigation on bioinformatics analysis of the SARS-CoV-2 S proteins, bioinformatics analysis of the S proteins encoded of SARS-CoV-2 genes was carried out, and the results were compared with SARS-CoV spike proteins. The homology modeling was also performed to estimate all possible protein structures, in which the interactions of RBD and CTD with ACE2, DPP4, CCR5, and AXL receptors were explored.

Method

To inhibit S protein, the binding of the S protein encoded with cellular receptors, *i.e.,* ACE2 [18], DPP4 [19], CCR5 [20-22], and AXL [23] was examined, and compared with S protein of SARS-CoV with ACE2 complex. Further, we evaluated the possible interaction and potential blocking of S protein encoded with cellular receptors.

Homology modeling of Spike protein

All genome sequences of SARS-CoV-2 S protein (NC_045512.2) were selected from the NCBI database. The nucleotide sequences were aligned through BLASTn to investigate the homology of SARS-CoV-2 genomes. Therefore, we found 32 sequences in GenBank via homology modeling.

The RBD and CTD structures were selected as active sites for the interaction with cellular receptors. The nucleotide sequence editing was carried out by the Bioedit program v7.0.5 [24], followed by aligning with ClustalW [25].

The evolutionary history was used as the Neighbor-Joining method via the MEGA-X [26]. The phylogenetic tree was generated through the JTT evolutionary model [27]. Homology modeling was performed through the Swiss-Model [28] based on most of sequences identity and coverage, which was superimposed over the template. The RMSD was investigated in Å via SWISS-PdBViewer 4.1.0 [29]. Structures generated were analyzed using UCSF Chimera [30,31].

Molecular docking

The molecular docking technique has been shown to be an accurate calculation to investigate the binding conditions of cellular receptors [32]. According to previous studies, DPP4 [19], CCR5 [20-22], and AXL [23] receptors serve as the key receptors for MERS-CoV, Human immunodeficiency (HIV), and Zika viruses, respectively. Considering the importance of RBD and CTD protein active pockets of SARS-CoV-2 in the virus infection [5], the interface binding of these active domains with the ACE2, DPP4, CCR5, and AXL cellular receptors were evaluated via molecular docking technique using HDOCK software [33]. The crystal structures were obtained employing the PDB for DPP4 (4L72), ACE2 (1R42), CCR5 (3ODU) and AXL (2C5D). In crystal structures reported, water molecules, ions, and ligands were removed to perform molecular docking protein-protein. Meanwhile, hydrogen atoms were added to better understand the hydrogen bonds of this study. The grid size of the system was equal to 72×76×62 and the distance between two grid points was set at 0.375 Å. The protein-protein docking was performed using a hybrid algorithm of *ab initio* free docking, which was then analyzed by the PRODIGY software [34]. The results were finally clustered and assessed based on both binding interacting energies and residues involved in complexes.

Molecular dynamic

In order to investigate the binding stability of the SARS-CoV-2 S protein active domains (RBD and CTD) with the receptors, molecular dynamic (MD) simulations were performed in an explicit solvent model based on GROMACS using GROMOS96 43a1 force field parameters [35,36]. The complex structures of the RBD and CTD interacted with the receptors were designed in water cube [37] with the simple point charge (SPC) water [38] model under the periodic boundary conditions, in which NaCl (0.154 M) was employed in the protein-water system to make the system electrostatically neutral. Our size of the system was equal to $10.70\times8.65\times6.61\ nm^3$. The structures of energy optimization were first performed using the steepest descent method [39] with a convergence criterion of $1000\ kj/mol\ nm^{-1}$. To make equilibration between the solvent, NaCl, and S protein-receptors complex, NVT and NPT ensemble were performed for 100 *ps* and a time-step of 2 *fs* at 300 *K* using Berendsen weak coupling method with 50000 steps. For NVT and NPT relaxation and energy minimization calculations, short-range interactions were constrained with a cutoff of 1.0 *nm*, and long-range electrostatics were constrained using the PME formalism [40]. The pressure was set at 1 bar by utilizing Parrinello-Rahman barostat. The simulation was performed using the LINCS algorithm for hydrogen bonds [41,42]. The MD simulation results were finally analyzed by GROMACS and Chimera software [43]. It is known that the system reaches equilibrium when the parameters, *e.g.,* energy and temperature, fluctuations fall within the range of 5%. Therefore, the equilibrium of the system is represented in Figure 1, in which Figures 1a and b represent the temperature and density profile versus the simulated time for SARS-CoV-2 RBD, SARS-CoV-2 CTD, and SARS-CoV RBD interacted with the ACE2 receptor
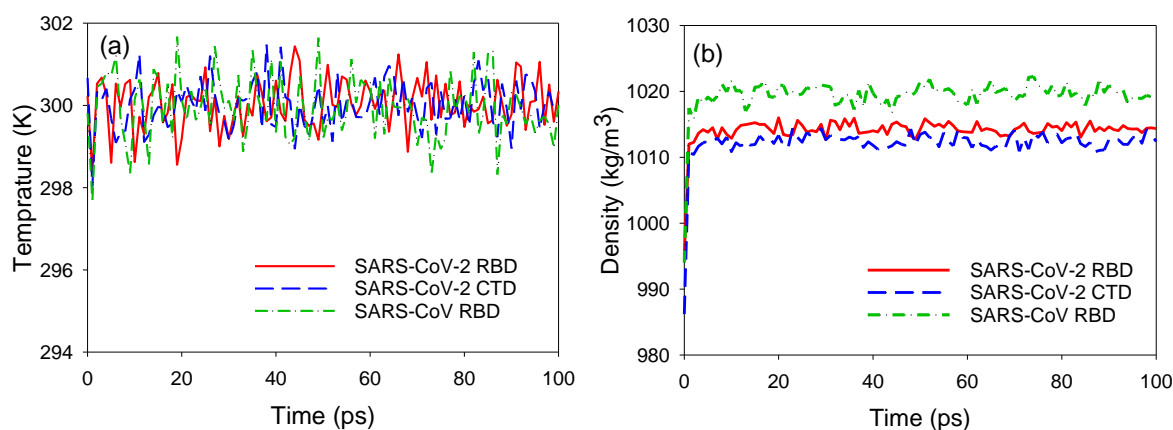

FIGURE 1 Temperatures and density versus simulation time for SARS-CoV-2 RBD, SARS-CoV-2 CTD, and SARS-CoV RBD interacted with ACE2 receptor

Results and discussion

Herein, we present *in silico* analyses of the binding affinities of the SARS-CoV-2 S protein active domains (RBD and CTD) to the cellular receptors (ACE2, DPP4, CCR5 and AXL), highlighting SARS-CoV-2 CTD-ACE2 and SARS-CoV-2 RBD-ACE2 complexes as interesting candidates for experimental evaluations.

Homology modeling of encoded SARS-CoV-2 proteins

Knowledge of protein 3D structure is a basic requirement for exploring the function of a protein. Homology modeling is the most standard *in silico* procedure that offers predicting the 3D structure of proteins using structural templates [44].

We obtained homology genomes based on the genome sequence of SARS-CoV-2/WHU02 that was aligned using the BLASTn online tool. Then, the phylogenetic results demonstrated a tree of 50 coronaviruses S protein, as shown in Figure 2a. We found three S proteins (97% for QIZ13861.1, QHU79173.2 and QJD20632.1) had the highest genome homology to the SARS-CoV-2 S protein. According to the recent study on SARS-CoV-2, SARS-CoV (80%) revealed the highest homology to SARS-CoV-2 [45]. SARS-CoV-2 RBD and CTD are the most

active sites according to previous literature [46,47]. In this study, we compared the sequence aligned of RBD and CTD in the S protein of SARS-CoV-2 with RBD of SARS-CoV (Figure 2b). The sequence alignment results revealed that 70% of the RBD and CTD sequence of SARS-CoV-2 homology was in contrast to SARS-CoV. Then, we aligned S protein RBD and CTD sequences from SARS-CoV-2 with the PDB database.
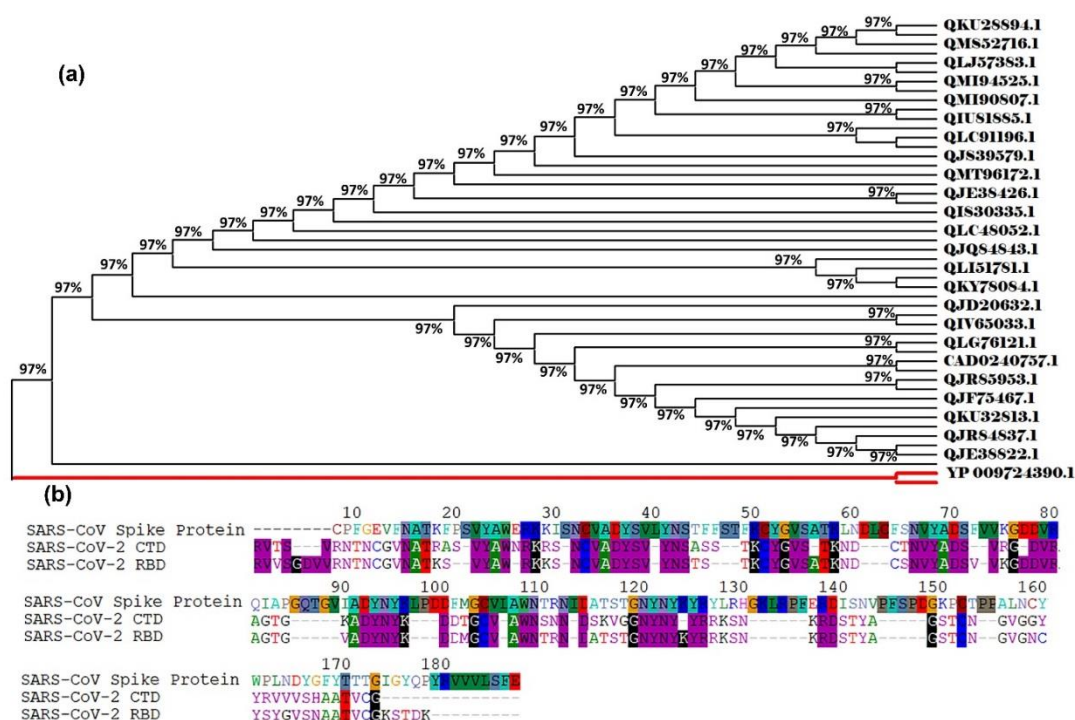

FIGURE 2 The phylogenetic tree analysis and sequence alignment of SARS-CoV-2 S protein. (a) The homology tree of 50 nucleotide sequences alignment. (b) The comparison between sequence alignment of the S proteins RBD/CTD from SARS-CoV-2 and SARS-CoV

Structural analyses of RBD- and CTD-receptors complexes

The homology modeling on the SARS-CoV-2 S protein RBD and CTD was obtained. Then, the crystal structures of the S protein RBD of SARS-CoV and homology models of SARS-CoV-2 RBD and CTD have been docked with different receptors such as ACE2, DPP4, CCR5 and AXL. The structural representation of the interaction of SARS-CoV-2 S protein RBD and CTD with ACE2, DPP4, CCR5 and AXL

receptors is shown in Figures 3 and 4. The molecular docking results exhibit that the best model was obtained using as a template the crystal structure PDB for S protein- ACE2 with code 6VW1 with 99.5% and 98.5% coverage for CTD and RBD, respectively. This crystal structure has been resolved via X-ray diffraction with a resolution of 2.68 Å [48]. In the case of SARS-CoV-2 S protein-DPP4, we selected the crystal structure (PDB: 4KR0) with 76.7% and 76.3 % coverage for CTD and RBD, respectively in which 4KR0 structure has

been resolved *via* X-ray diffraction with a resolution of 2.70 Å [49]. The best models selected for RBD/CTD-CCR5 complex are 5DSG (receptor) and 6VW1 (RBD/CTD) with 99.5% and 98.5% coverage for CTD and RBD, respectively. The crystal structure PDB: 6XC3 is as the best model for RBD/CTD-AXL complex with 87.6% and 87.3% coverage for CTD and RBD, respectively.

Molecular docking

In this section, molecular docking analyses from the binding of RBD and CTD with the cellular receptors have been presented. The binding energy is due to the energies contributed by residues in the interface of target proteins. The residues energies are due to interactions, *i.e.,* hydrogen bonding, π-π stacking, etc. [50]. The human ACE2 receptor is a protein with two main domains including NPD and CTD [13]. Therefore, the binding of ACE2 and S protein includes interaction sites active of S protein (RBD and CTD) and the ACE2 peptidase domain (PD). There are short loop-interface interactions that may play as a bridge in binding the S protein and the ACE2.
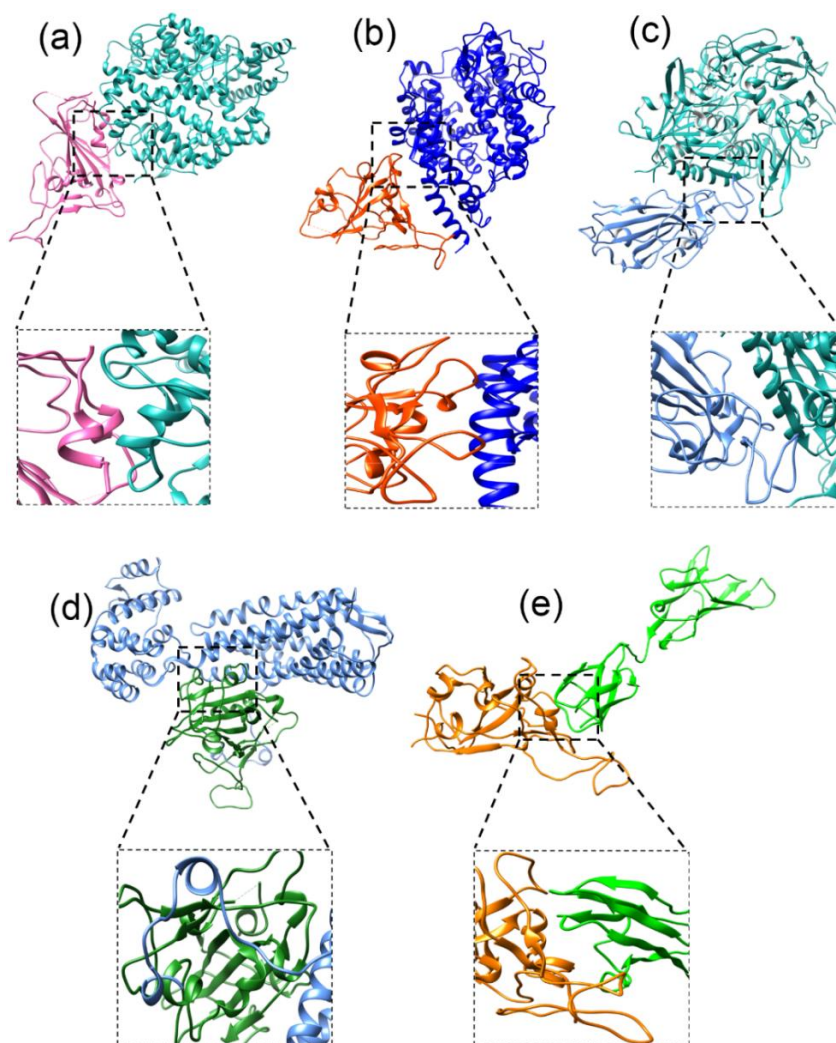

FIGURE 3 Three-dimensional schematic of SARS-CoV-2 CTD with the receptors. (a) Complex of ACE2 and SARS-CoV-2 CTD, where ACE2 and CTD are shown in green and pink, respectively. (b) The protein of ACE2 and SARS-CoV, where ACE2 and SARS-CoV are shown in orange and blue, respectively. (c) The complex of DPP4 and SARS-CoV-2 CTD, where DPP4 and CTD are shown in green and pale blue, respectively. (d) Complex of CCR5 and SARS-CoV-2 CTD, where CCR5 and CTD are shown in blue and green, respectively. (e) Simulation of AXL and SARS-CoV-2 CTD, where AXL and CTD are shown in orange and green, respectively
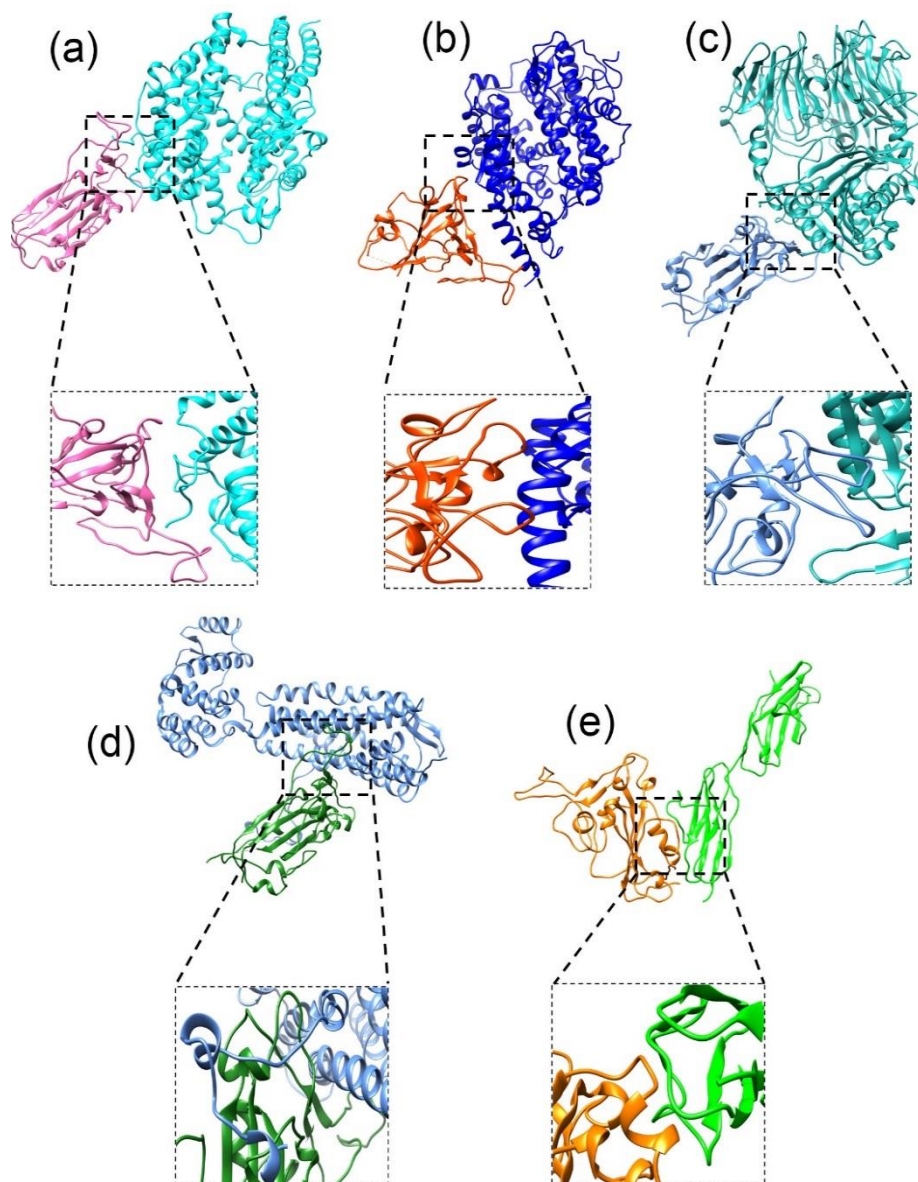
FIGURE 4 Three-dimensional view of SARS-CoV-2 RBD with the receptors. (a) Structure of ACE2 and SARS-CoV-2 RBD, where ACE2 and RBD are shown in green and pink, respectively. (b) The complex of ACE2 and SARS-CoV, where ACE2 and SARS-CoV are shown in orange and blue, respectively. (c) The protein of DPP4 and SARS-CoV-2 RBD, where DPP4 and RBD are shown in green and pale blue, respectively. (d) Simulation of CCR5 and SARS-CoV-2 RBD, where CCR5 and RBD are shown in blue and green, respectively. (e) The complex of AXL and SARS-CoV-2 RBD, where AXL and RBD are shown in orange and green, respectively

We found that SARS-CoV-2 CTD-ACE2 (-15.3 $kcal/mol$) was capable of being helpful for viral infection treatment. Similarly, SARS-CoV-2 RBD was investigated as the second-lowest binding affinity (-12.5 $kcal/mol$) for SARS-CoV-2 S protein compared with SARS-CoV (-11.4 $kcal/mol$) as shown in Figure 5a. The stability of the system using the equilibrium dissociation constant ($K_d =$ $[L]_{eq}[P]_{eq}/[PL]_{eq}$ which $[L]_{eq}$, $[P]_{eq}$ and $[PL]_{eq}$ are equilibrium concentrations of ligand, protein and protein-ligand) [51] as illustrated in Figure (5b). The dissociation constant has a key role to design adequate models for systems biology and ranking pharmaceutical in drug delivery.

Our results were consistent with the previous prediction for protein-protein

docking of SARS-CoV-2 spike RBD and ACE2 [52]. The connected residues in the binding SARS-CoV-2 spike protein CTD-ACE2 and SARS-CoV-ACE2 are illustrated in Table 1. It is observed that the residues such as Asn25, Asp46, Asn16, and Pro209 act as a salt bridge between SARS-CoV-2 CTD and ACE2. In comparison to SARS-CoV, they are different which residues, *e.g.,* Gln175, Gln180, Tyr131, Thr182, Phe168, Asn183, and Tyr171 with ACE2 are involved
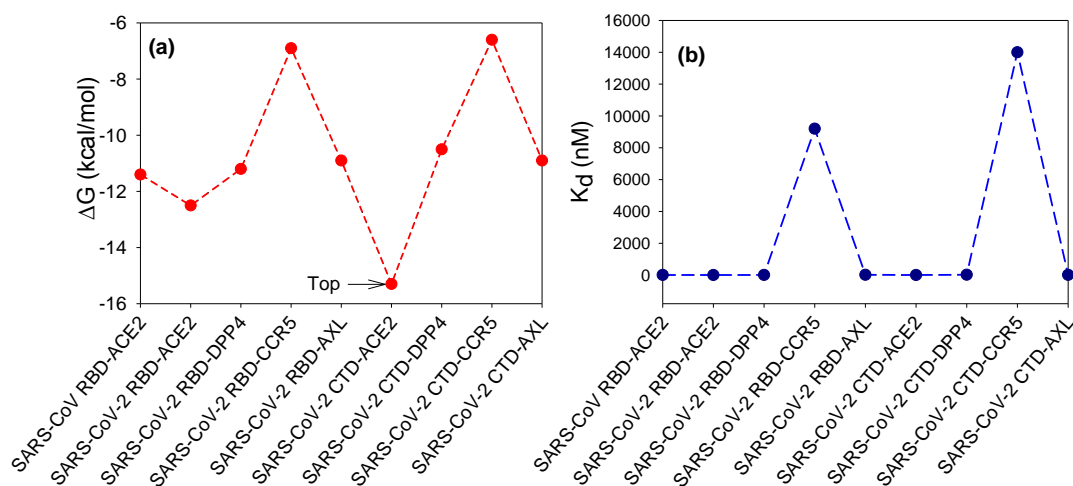

FIGURE 5 Binding affinity (ΔG) and dissociation constant (K_d) for the binding between SARS-CoV-2 RBD/CTD and the receptors

The microenvironment of the ACE2 receptor allows those amino acids in the active site to interact efficiently and produce a significant amount of minimum electrostatic stabilizing interactions. Meanwhile, there are short loops in the interaction sites active of S protein with the cellular receptor which these loops cause stability in the complex. We found these loops in our structures, though they were weak (Table 1). These results are due to the presence of hydrogen bonding between the proteins [53].

TABLE 1 Residues involved in the interactions of SARS-CoV-2 spike protein CTD-ACE2 and SARS-CoV-ACE2

SARS-CoV-2 CTD-ACE2		SARS-CoV RBD-ACE2	
ACE2	S protein	ACE2	S protein
Ala246-ASN250- MET249- Pro258.	Gly21	Ser254-Ser611-Ser257- Trp610-Ile256-Tyr255- Pro612-Tyr613.	Gln175
Pro253-Asn250-Met249.	Phe24	Ser254	Val99
Tyr255- Met249- Ala246- Arg245- Asn250- Leu248- Ile256- Ala251- Pro253- Tyr252- Ser257- Ser254- Pro258.	Asn25	Asn601-Ser602.	Gly184
Pro253-Leu156 Asn250- Ala251- Tyr252 Lys247- Met249.	Ser53	Pro258-Gly 260- Ile259- Ser607-Phe603.	Gln180
Asn250- Ser280- Ala246- Ala251- Leu248- Leu281.	Val49	Val491-Pro492.	Gly167
Thr282- Gly286- Lys247- Val283- Ser280- Leu281.	Ser48	Pro492-Ala614-Tyr613.	Glu166

Tyr255-Ser254.	Ile123	Ile259- Trp610- Ser257- Ser607- Gly260.	Tyr131
Gln598- Lys247-Tyr243- Asp597- Asn601.	Leu17	Met249- Pro258-Asn250- Ala246.	Tyr187
Thr282- Lys247- Val283- Pro284- Tyr243- Gly286- Leu281-Asn250	Asp46	Leu162-Val491-Trp163 - Pro135.	Asn169
Tyr158- Tyr252- Pro253- Leu156-Asp157- Ser254- Ala251.	Phe55	Ile259- Pro258.	Phe179
Gln598- Phe285.	Val44	Ser602- Phe603- Val604- Lys600 - Asn601.	Thr182
Glu433-Pro284-Gln287- Phe285-Tyr255-Gly286.	Pro209	Ser167- Pro135-Trp163- Tyr497- Glu166-Ala164- Ser170Leu162-Val491.	Phe168
Gln287-Phe285-Gly286.	Asn70	Ser257-Pro258- Ile259	Gly178
Lys247.	Tyr47	Ile259-Asn601- Pro258- Phe603-Ser602.	Asn183
Ser254-Pro253.	Trp118	Tyr158-Pro490- Val491- Trp163-Leu162- Asn159.	Tyr171
Asn159- Tyr255.	Asn122	Asn159- Tyr158 - Tyr255.	Phe138
Asn601.	Cys18	Pro135	Ser159
Pro253- Asn250- Ala251.	Phe56	Ser257- Trp610.	Ser176
Ala251-Leu156- Leu281- Ser280	Asn52	Tyr613-Pro612-Ala614.	Phe172
Asp597-Lys596-Asn601- Lys600- Gln598.	Asn16	Tyr255-Ser254-Ile256.	Tyr135
Ser254	Val23	Ser257- Pro258.	Tyr177
Leu156	Thr54	Ser254 -Tyr255- Pro253.	Leu137
Gly286	Tyr51	Asn601	Val185
Pro258	Thr27	Ser607	Thr128
Asn601- Met249.	Glu22	Tyr613-Ala614.	Leu174
Gln287	Asp71	Phe603	Ser127
Asn250	Phe20	Ile259	Asn130
Asn250-Ala251-Pro253.	Leu50	Ile259	Gly129
Gln287-Phe285.	Gly208		
Ser254-Ile256.	Ala26		
Asn601	Pro19		
Ser254	Thr120- Phe29- Phe24- Arg191		
Tyr255	Asn119		

The hydrophobicity and the complementarity shape of the receptors and RBD/CTD have a crucial role in the inhibiting of the S protein [54]. As a result, these loops and mutations are capable of playing a key role in blocking interface S protein and receptors (see Table 1). The detail of interface binding RBD/CTD to receptors, *i.e.,* ACE2, DPP4, CCR5, and AXL cellular receptors, were evaluated (Figures 6 and 7). The binding of cellular receptors in the active residues of CTD is shown in Figures 6. Moreover, in Figure 7 we observed the contact residues of the interface RBD-receptors.
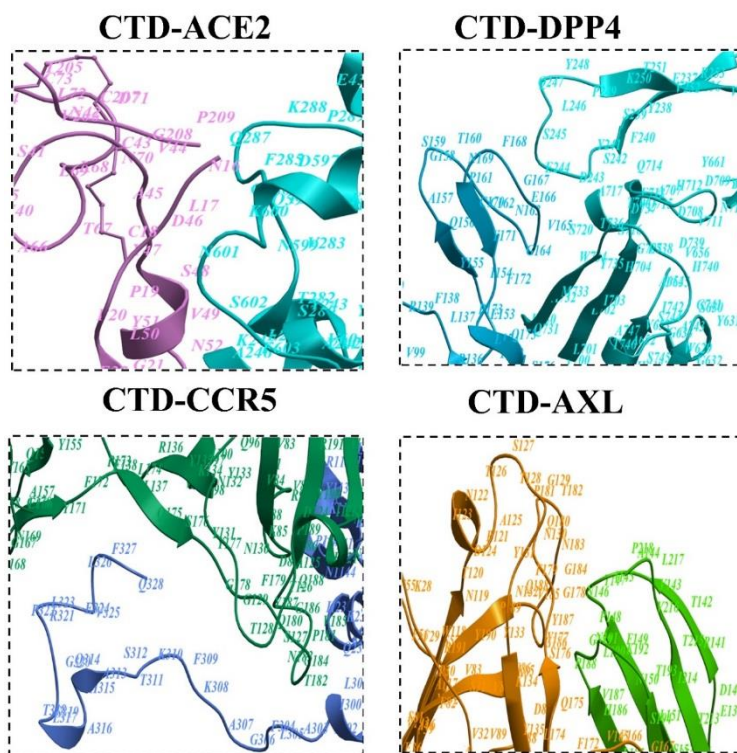
CTD-ACE2

CTD-DPP4

CTD-CCR5

CTD-AXL

FIGURE 6 The structure of the residues between SARS-CoV-2 S1/CTD and ACE2 with histrelin (in the pocket of ligand) in comparison to SARS-CoV RBD. The ACE2 is in blue, the core of S1/CTD is in yellow
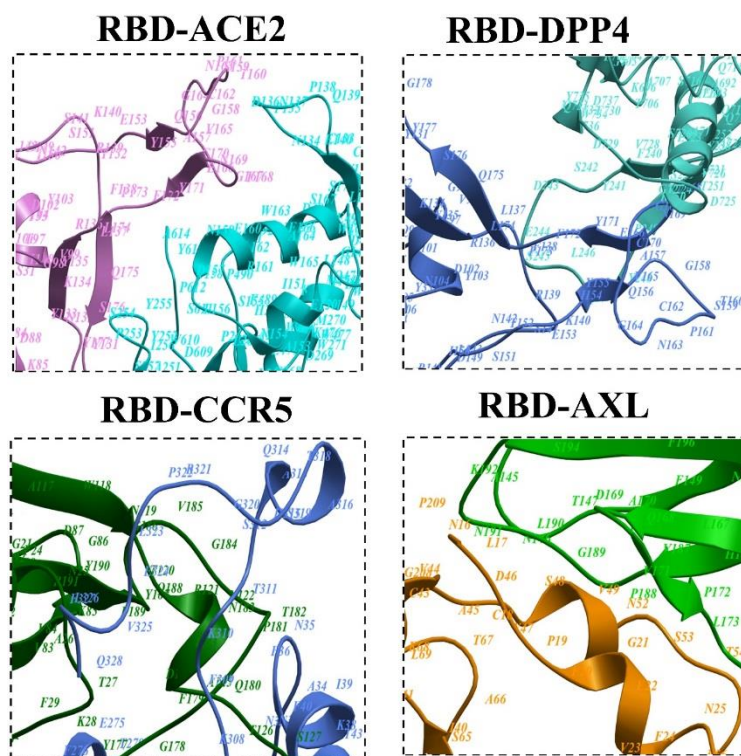
RBD-ACE2

RBD-DPP4

RBD-CCR5

RBD-AXL

FIGURE 7 The structure of the interface between SARS-CoV-2 S1/CTD and ACE2 with histrelin (in pocket of ligand) in comparison to SARS-CoV RBD. The ACE2 is in blue, the core of S1/CTD is in yellow

Table 2 reveals the protein-protein contacts SARS-CoV-2 and SARS-CoV spikes and receptors.

TABLE 2 The protein-protein contacts between SARS-CoV-2 and SARS-CoV S proteins and receptors

Protein-protein complex	Charged-charged	Charged-polar	Charged-apolar	Polar-polar	Polar-apolar	Apolar-apolar
SARS-CoV RBD-ACE2	1	9	19	2	18	8
SARS-CoV-2 RBD-ACE2	0	1	4	10	37	36
SARS-CoV-2 RBD-DPP4	2	14	19	12	24	20
SARS-CoV-2 RBD-CCR5	3	18	8	4	12	32
SARS-CoV-2 RBD-AXL	1	14	6	11	30	19
SARS-CoV-2 CTD-ACE2	1	10	12	12	46	30
SARS-CoV-2 CTD-DPP4	6	14	17	13	21	22
SARS-CoV-2 CTD CCR5	3	18	8	4	11	32
SARS-CoV-2 CTD-AXL	2	5	12	13	29	29

Molecular dynamics

Molecular dynamics (MD) simulation is a great tool to understand the structure-to-function relevance of a protein and its corresponding physical transitions of atoms [55,56]. This technique is also a suitable method to study the properties of protein-protein interactions [57]. Utilizing an MD simulation, one of the results afforded is linked to the radius of gyration (R_g), which is an interesting way to explore the folding and compactness properties of protein-protein complexes [58]. The high R_g value reveals a structure of S protein-receptors with loose packing, while a smaller R_g value represents S protein-receptors with tight packing. Therefore, the radius of gyration can be employed to investigate the folding behavior of a protein after docking to a receptor. In the case of SARS-CoV-2, the RBD-DPP4 complex exhibits more compact than the separate S protein and receptors (Figure 8). The average R_g values of CTD-ACE2, RBD-ACE2 and RBD-AXL complex were obtained to be 3.175 nm, 3.181 nm, and 3.244 nm, respectively, compared with 3.058 nm for SARS-CoV.
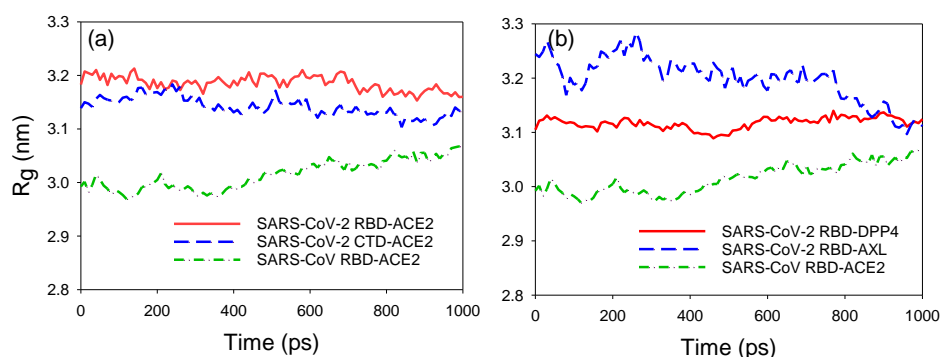

FIGURE 8 Radius of gyration (R_g) versus time for SARS-CoV-2 CTD/RBD with the receptors. (a) Radius of gyration for SARS-CoV-2 CTD and RBD ACE2 (blue and red) compared to SARS-CoV RBD-ACE2 (green), respectively. (b) Radius of gyration for SARS-CoV-2 RBD DPP4 (red) and AXL (blue) compared to SARS-CoV RBD-ACE2 (green), respectively

Conclusion

We theoretically evaluated the interactions of two active sites (RBD and CTD) of SARS-CoV-2 spike protein with the cellular receptors including ACE2, DPP4, CCR5, and AXL. Binding affinities of eight possible RBD/CTD-receptor complexes were investigated via a high throughput protein-protein docking strategy. The results revealed that the SARS-CoV-2 has strong binding capabilities to ACE2, but weaker than that of SARS-CoV S protein. The presence of capping loops in the S protein RBD/CTD could be one of the reasons enhancing binding to the receptors. The homology modeling and *in silico* study provided three major results. First, protein products of SARS-CoV-2 S protein-encoding gene sequences are not only related to the binding affinity to the ACE2 but also to improve this receptor recognition. The second result is the loops observed from RBD/CTD to receptors could play an important role to determine the host receptor specificity for the viral S protein and control of SARS-CoV-2 infection. We highlighted the residues such as Asn25, Asp46, Asn16, and Pro209 as a salt bridge in the interface of CTD-ACE2. The third result the binding to RBD with receptors (DPP4 and AXL) might provide promising information for SARS-CoV-2 inhibition. In conclusion, our results suggest that encoding the active sites of spike protein has the capability to block SARS-CoV-2 from binding to the cellular ACE2 and may reduce the invasion ability of the virus.

Acknowledgments

Orcid:

Saeedeh Mohammadi: https://orcid.org/0000-0003-2204-3661
Esmail Doustkhah:
https://www.orcid.org/0000-0003-1459-1756
Ahmad Reza Salehi Chaleshtori:
https://orcid.org/0000-0002-8689-8450
Mohammad Esmailpour:
https://orcid.org/0000-0001-9086-0941
Farzad Zamani: https://orcid.org/0000-0001-8469-6364
Ayoub Esmailpour: https://orcid.org/0000-0001-8340-7348

References

[1] C. Wang, P.W. Horby, F.G. Hayden, G.F. Gao, *Lancet.*, **2020**, *395*, 470-473. [crossref], [Google Scolar], [Publisher]

[2] P.J. Lillie, A. Samson, A. Li, K. Adams, R. Capstick, G.D. Barlow, N. Easom, E. Hamilton, P.J. Moss, A. Evans, M. Ivan, PHE Incident Team, Y.Taha, C.J.A. Duncan, M.L. Schmid, the Airborne HCID Network, *J. Infect.*, **2020**, *80*, 578-606. [crossref], [Google Scolar], [Publisher]

[3] Q. Li, X. Guan, P. Wu, X. Wang, L. Zhou, Y. Tong, *et al.*, *N. Engl. J. Med.*, **2020**, *382*, 1199-1207. [crossref], [Google Scolar], [Publisher]

[4] J. Lan, J. Ge, J. Yu, S. Shan, H. Zhou, S. Fan, Q. Zhang, X. Shi, Q. Wang, L. Zhang, X. Wang, *Nature.*, **2020**, *581*, 215-220. [crossref], [Google Scolar], [Publisher]

[5] B. Hu, H. Guo, P. Zhou, Z.-L. Shi, *Nat. Rev. Microbiol.*, **2020**. *19*, 141–154. [crossref], [Google Scholar], [Publisher]

[6] M. Lotfi, N. Rezaei, *J. Med. Virol.*, **2020**, *92*, 1864-1874. [crossref], [Google Scholar], [Publisher]

[7] World Health Organization. 2020. Available online: https://covid19.who.int/ (accessed on 12 March 2021). [crossref], [Google Scolar], [Publisher]

[8] G. Lu, D. Liu, *Protein Cell.*, **2012**, *3*, 803-805. [crossref], [Google Scholar], [Publisher]

[9] Q. Wang, Y. Zhang, L. Wu, S. Niu, C. Song, Z. Zhang, G. Lu, C. Qiao, Y. Hu, K.Y. Yuen, Q. Wang, H. Zhou, J. Yan, J. Qi, *Cell,* **2020***, 181*, 894-904. [crossref], [Google Scholar], [Publisher]

[10] W. Li, *Biophys. Chem.*, **2020**, *264*, 106420. [crossref], [Google Scholar], [Publisher]

[11] K. Ziaa, S. Ali Khana, S. Ashraf, M. Nur-e-Alamb, S. Ahmedb, Z. Ul-Haq, *J. Mol. Struct.*,

2021, *1231*, 129953. [[crossref]], [[Google Scholar]], [[Publisher]]

[12] M. Hussain, N. Jabeen, F. Raza, S. Shabbir, A.A. Baig, A. Amanullah, B. Aziz, *J. Med. Virol.*, **2020**, *92*, 1580-1586. [[crossref]], [[Google Scholar]], [[Publisher]]

[13] K. Kuba, Y. Imai, S. Rao, H. Gao, F. Guo, B. Guan, Y. Huan, P. Yang, Y. Zhang, W. Deng, L. Bao, B. Zhang, G. Liu, Z. Wang, M. Chappell, Y. Liu, D. Zheng, A. Leibbrandt, T. Wada, A.S. Slutsky, D. Liu, C. Qin, C. Jiang, J.M. Penninger, *Nat. Med.*, **2005**, *11*, 875-879. [[crossref]], [[Google Scolar]], [[Publisher]]

[14] J.S. Jerng, Y.C. Hsu, H.D. Wu, H.Z. Pan, H.C. Wang, C.T. Shun, C.J. Yu, P.C. Yang, *Thorax.*, **2007**, *62*, 527-535. [[crossref]], [[Google Scolar]], [[Publisher]]

[15] L.N. Chen, X.H. Yang, D.H. Nissen, Y.Y. Chen, L.J. Wang, J.H. Wang, J.L. Gao, L.Y. Zhang, *Shock.*, **2013**, *40*, 420-429**.** [[crossref]], [[Google Scholar]], [[Publisher]]

[16] K. Kuba, Y. Imai, S. Rao, H. Gao, F. Guo, B. Guan, Y. Huan, P. Yang, Y. Zhang, W. Deng, L. Bao, B. Zhang, G. Liu, Z. Wang, M. Chappell, Y. Liu, D. Zheng, A. Leibbrandt, T. Wada, A.S. Slutsky, D. Liu, C. Qin, C. Jiang, J.M. Penninger, *Nat. Med.*, **2005**, *11*, 875-879. [[crossref]], [[Google Scholar]], [[Publisher]]

[17] S. Mohammadi, M. Heidarizadeh, M. Entesari, A. Esmailpour, M. Esmailpour, R. Moradi, N. Sakhaee, E. Doustkhah, *Microorganisms.*, **2020**, *8*, 1600. [[crossref]], [[Google Scholar]], [[Publisher]]

[18] P. Towler, B. Staker, B., S.G. Prasad, S. Menon, J. Tang, T. Parsons, D. Ryan, M. Fisher, D. Williams, N.A. Dales, M.A. Patane, M.W. Pantoliano, *J. Biol. Chem.*, **2004**, *279*, 17996-18007. [[crossref]], [[Google Scholar]], [[Publisher]]

[19] V.S. Raj, H. Mou, S.L. Smits, D.H.W. Dekkers, M.A. Müller, R. Dijkman, D. Muth, J.A.A. Demmers, A. Zaki, R.A.M. Fouchier, V. Thiel, C. Drosten, P.J.M. Rottier, A.D.M.E. Osterhaus, B.J. Bosch, B.L. Haagmans, *Nature.*, **2013**, *495*, 251-254. [[crossref]], [[Google Scholar]], [[Publisher]]

[20] G.B. Melikyan, *Retrovirology.*, **2008**, *5*, 111. [[crossref]], [[Google Scholar]], [[Publisher]]

[21] G. Alkhatib, *Curr. Opin. HIV AIDS.*, **2009**, *4*, 96-103. [[crossref]], [[Google Scholar]], [[Publisher]]

[22] R.W. Doms, *J. Immunol.*, **2011**, *186*, 6073-6075. [[crossref]], [[Google Scholar]], [[Publisher]]

[23] T.J. Nowakowski, A.A. Pollen, E. Di Lullo, C. Sandoval-Espinosa, M. Bershteyn, A.R. Kriegstein, *Cell. Stem. Cell.*, **2016**, *18*, 591-596. [[crossref]], [[Google Scholar]], [[Publisher]]

[24] H.-F. Tippmann, *Briefings in Bioinform.*, **2004**, *5*, 82-87. [[crossref]], [[Google Scholar]], [[Publisher]]

[25] J.D. Thompson, T.J. Gibson, D.G. Higgins, *Current protocols. Bioinform.*, **2003**, *1*, 2-3. [[crossref]], [[Google Scholar]], [[Publisher]]

[26] S. Kumar, G. Stecher, M. Li, C. Knyaz, K. Tamura, *Mol. Biol. Evol.*, **2018**, *35*, 1547-9. [[crossref]], [[Google Scholar]], [[Publisher]]

[27] D.T. Jones, W.R. Taylor, J.M. Thornton, *Comput. Appl. Biosci.*, **1992**, *8*, 75-82. [[crossref]], [[Google Scholar]], [[Publisher]]

[28] A. Waterhouse, M. Bertoni, S. Bienert, G. Studer, G. Tauriello, R. Gumienny, F.T. Heer, T.A.P. de Beer, C. Rempfer, L. Bordoli, R. Lepore, T. Schwede, *Nucleic Acids Res.*, **2018**, *46*, W296-W303. [[crossref]], [[Google Scholar]], [[Publisher]]

[29] M.U. Johansson, V. Zoete, O. Michielin, N. Guex, *BMC Bioinform.*, **2012**, *13*, 173. [[crossref]], [[Google Scholar]], [[Publisher]]

[30] E. Pettersen, T. Goddard, C. Huang, G. Couch, D. Greenblatt, E. Meng, T. Ferrin, *J. Computat. Chem.*, **2004**, *25*, 1605. [[crossref]], [[Google Scholar]], [[Publisher]]

[31] R.C. Edgar, B.J. Haas, J.C. Clemente, C. Quince, R. Knight, *Bioinformatics.*, **2011**, *27*, 2194-2200. [[crossref]], [[Google Scholar]], [[Publisher]]

[32] G. Morris, R. Huey, W. Lindstrom, M. Sanner, R. Belew, D. Goodsell, A. Olson, *J. Comput. Chem.*, **2009**, *30*, 2785. [[crossref]], [[Google Scholar]], [[Publisher]]

[33] Y. Yan, H. Tao, J. He, S.Y. Huang, *Nat. Protoc.*, **2020**, *15*, 1829-1852. [crossref], [Google Scholar], [Publisher]

[34] L.C. Xue, J.P. Rodrigues, P.L. Kastritis, A.M. Bonvin, A. Vangone, *Bioinformatics.*, **2016**, *32*, 3676-3678. [crossref], [Google Scholar], [Publisher]

[35] E. Lindahl, B. Hess, D. van der Spoel, *J. Mol. Model.*, **2001**, *7*, 306-317. [crossref], [Google Scholar], [Publisher]

[36] S.-W. Chiu, S.A. Pandit, H.L. Scott, E. Jakobsson, *J. Phys. Chem. B.*, **2009**, *113*, 2748-2763. [crossref], [Google Scholar], [Publisher]

[37] H.J.C. Berendsen, J.R. Grigera, T.P. Straatsma, *J. Phys. Chem.*, *1987*, **91**, 6269-6271. [crossref], [Google Scholar], [Publisher]

[38] H.J.C. Berendsen, J.P.M. Postma, W.F. van Gunsteren, J. Hermans, *In Intermolecular Forces*; Pullman, B., Ed.; Reidel: Dordrecht. **1981**, *331-342*. [crossref], [Google Scholar], [Publisher]

[39] H.J.C. Berendsen, J.P.M. Postma, W.F.v. Gunsteren, A. DiNola, J.R. Haak, *J. Chem. Phys.*, **1984**, *81*, 3684-3690. [crossref], [Google Scholar], [Publisher]

[40] A. Toukmaji, C. Sagui, J. Board, T. Darden, *J. Chem. Phys.*, **2000**, *113*, 10913-10927. [crossref], [Google Scholar], [Publisher]

[41] B. Hess, H. Bekker, H.J.C. Berendsen, J.G.E.M. Fraaije, *J. Comput. Chem.*, **1997**, *18*, 1463-1472. [crossref], [Google Scholar], [Publisher]

[42] B. Hess, *J. Chem. Theory Comput.*, **2008**, *4*, 116-22. **[**crossref], [Google Scholar], [Publisher]

[43] E.F. Pettersen, T.D. Goddard, C.C. Huang, G.S. Couch, D.M. Greenblatt, E.C. Meng, T.E. Ferrin, *J. Comput. Chem.*, **2004**, *25*, 1605-1612. [crossref], [Google Scholar], [Publisher]

[44] L. Bordoli, F. Kiefer, K. Arnold, P. Benkert, J. Battey, T. Schwede, *Nat. Protoc.*, **2009**, *4*, 1-13. [crossref], [Google Scholar], [Publisher]

[45] P. Zhou, X.-L. Yang, X.-G. Wang, B. Hu, L. Zhang, W. Zhang, et al. *Nature*, **2020**, *579*, 270-273. [crossref], [Google Scholar], [Publisher]

[46] D. Wrapp, N. Wang, K.S. Corbett, J.A. Goldsmith, C.L. Hsieh, O. Abiona, B.S. Graham, J.S. McLellan, *Science*, **2020**, *367*, 1260-1263. [crossref], [Google Scholar], [Publisher]

[47] R. Yan, Y. Zhang, Y. Li, L. Xia, Y. Guo, Q. Zhou, *Science*, **2020**, *367*, 1444-1448. [crossref], [Google Scholar], [Publisher]

[48] J. Shang, G. Ye, K. Shi, Y. Wan, C. Luo, H. Aihara, Q. Geng, A. Auerbach, F. Li, *Nature*, **2020**, *581*, 221-224. [crossref], [Google Scholar], [Publisher]

[49] a) G. Lu, Y. Hu, Q. Wang, J. Qi, F. Gao, Y. Li, Y. Zhang, W. Zhang, Y. Yuan, J. Bao, B. Zhang, Y. Shi, J. Yan, G.F. Gao, *Nature*, **2013**, *500*, 227-231. [crossref], [Google Scholar], [Publisher]; b) S.V. Gaikwad, M. V. Gaikwad, P. D. Lokhande, *J. Appl. Organomet. Chem.*, **2021**, *1*, 1-8. [crossref], [Google Scholar], [Publisher], [Download Pdf]

[50] D. Kumara, K. Kumari, A. Jayaraj, V. Kumar, R.V. Kumar, S.K. Dass, R. Chandra, P. Singh, *J. Biomol. Struct. Dyn.*, 2020. [crossref], [Google Scholar], [Publisher]

[51] Z.X. Wang, N.R. Kumar, D.K. Srivastava, *Analytical Biochem.*, **1992**, *206*, 376-381. [crossref], [Google Scholar], [Publisher]

[52] X. Xu, P. Chen, J. Wang, J. Feng, H. Zhou, X. Li, W. Zhong, P. Hao, *Sci. China Life Sci.*, **2020**, *63*, 457-460. [crossref], [Google Scholar], [Publisher]

[53] R.J. Khan, R.K. Jha, G.M. Amera, M. Jain, E. Singh, A. Pathak, R.P. Singh, J. Muthukumaran, A.K. Singh, *J. Biomol. Struct. Dyn.*, **2020**. *39*, 2679-2692. [crossref], [Google Scholar], [Publisher]

[54] C.A. MacRaild, A.H. Daranas, A. Bronowska, S.W. Homans, *J. Mol. Biol.*, **2007**, *368*, 822-832. [crossref], [Google Scholar], [Publisher]

[55] P. Ambure, J. Bhat, T. Puzyn, K. Roy, *J. Biomol. Struct. Dyn.*, **2018**, *37*, 1282-1306. [crossref], [Google Scholar], [Publisher]

[56] G.M. Amera, R.J. Khan, A. Pathak, R.K. Jha, J. Muthukumaran, A.K. Singh, *J. Biomol. Struct. Dyn.*, **2019**, *38*, 5230-5252. [crossref], [Google Scholar], [Publisher]

[57] G.M. Amera, R.J. Khan, A. Pathak, A. Kumar, A.K. Singh, *Inform. Med. Unlocked,* **2019**, *16*, 100216. [crossref], [Google Scholar], [Publisher]

[58] M.Y. Lobanov, N.S. Bogatyreva, O.V. Galzitskaya, *Mol. Biol.*, **2008**, *42*, 623-628. [crossref], [Google Scholar], [Publisher]